Available online at www.sciencedirect.com
SCIENCE DIRECT®
International Journal of Mass Spectrometry 227 (2003) 577–585
International Journal of Mass Spectrometry
www.elsevier.com/locate/ijms

Comparison of methyl and hydroxyl protons generated in a Coulomb explosion event: application of a time-of-flight gating technique to methanol clusters

Eric S. Wisniewski [a], A. Welford Castleman Jr. [a,b,*]

[a] *Department of Chemistry, The Pennsylvania State University, University Park, PA 16802, USA*
[b] *Departments of Chemistry and Physics, The Pennsylvania State University, University Park, PA 16802, USA*

Received 24 April 2002; accepted 12 September 2002

Abstract

A time-of-flight (TOF) mass spectrometry gating technique is applied to a study of methanol clusters subjected to ionizations via intense femtosecond laser pulses. The resulting high charged species (C^{2+}, C^{3+}/O^{4+}) acquire large amounts of kinetic energy resulting from Coulomb repulsion of multicharged atomic ions that reside in close proximity to one another. Protons which are of two kinds, methyl and hydroxyl, also acquire large amounts of kinetic energy. When compared with protons generated from the Coulomb explosion of water clusters ($(H_2O)_n$, $n \leq 20$), protons from methanol clusters ($(CH_3OH)_n$, $n \leq 10$) acquire less overall average kinetic energy, which is in agreement with earlier findings that suggest greater clustering yields higher energy. Interestingly, despite the lower average kinetic energy released, the methanol protons peak at a higher value of energy than those generated in the water cluster system, an effect attributed to the presence of both methyl and hydroxyl groups.

Keywords: Dynamical studies; Coulomb explosion; Energetic fragments; Femtosecond dynamics; Clusters

1. Introduction

The advent of femtosecond laser systems has allowed for the investigation of dynamical studies with the established pump-probe technique; the short pulse durations allow for time resolutions that yield data on intermediate reaction states [1,2]. A series of investigations with femtosecond laser systems that has received less attention takes advantage of the high powers and strong fields generated [3–6]. Of particular interest is the phenomenon termed Coulomb explosion where short time, high power laser pulses can lead to multicharged, highly energetic fragments born from atomic and molecular cluster systems [7–9]. As a result of this unique phenomenon, Coulomb explosion has evoked increasing interest from the scientific community.

Highly energetic atomic fragments produced in a Coulomb explosion event arise from the close proximity of positively charged ion cores. The molecular and cohesive bonds disintegrate as the electrons are removed on a femtosecond timescale. This time scale is too fast for appreciable atomic rearrangement to occur and the like-charges convert their potential energy to kinetic energy. Translational energies into the MeV realm have been observed for various fragments [10,11].

* Corresponding author. Tel.: +1-814-865-7242; fax: +1-814-865-5235.
E-mail address: awc@psu.edu (A.W. Castleman Jr.).

1387-3806/03/$ – see front matter © 2003 Elsevier Science B.V. All rights reserved.
doi:10.1016/S1387-3806(03)00093-9

The repelled atomic ions accelerate in all directions following the Coulomb explosion event. When this process is initiated in a time-of-flight mass spectrometer, only those fragments that are accelerated along the axis of the spectrometer are able to be detected, with all others careening off at angles that do not allow detection. Ions ejected along the axis of the mass spectrometer can become directed toward and away from the detector. These two moieties lead to a characteristic peak shape in the mass spectrum. Forward-ejected species reach the detector in a broad range of energies (assuming their energy, given by the birth potential plus the kinetic energy, does not exceed the potential placed upon the reflectron) while backward-ejected species (assuming the field placed upon TOF_1 exceeds the birth potential plus the kinetic energy) can be turned around and focused to arrive at the detector at a later time as a sharper peak. The average kinetic energy released has been calculated with two independent methods: the peak splitting and cut-off methods [6]. Each method possesses shortcomings that may lead to the determination of incorrect average kinetic energy release values.

Most recently, a new method was developed that enabled the investigation of multicharged atomic ions resulting from the Coulomb explosion of water clusters as a function of kinetic energy [12]. The method allows study of species with very large well-defined KER ranges by quantitatively lowering the energy of the highly energetic species so that they may be detected. By gating certain energy ranges, the total kinetic energy distribution can be obtained up to a limit imposed by the maximum potentials which can be applied to the various electrical lenses of the mass spectrometer. The gating method considerably extends the magnitude of the kinetic energies which can be studied compared to the more conventional techniques utilized in past studies.

In earlier work in our laboratory, water clusters were subjected to intense optical fields provided by an amplified femtosecond laser system. Multicharged atomic ions O^{2+}, O^{3+} and O^{4+}, as well as H^+ and O^+ atoms, were shown to be produced during the event. While the O^{2+} and O^{3+} atoms displayed a discontinuous range of kinetic energy values, the O^{4+} atom was not dominated by a particular range but rather, was found to be present in a wide range of energies. This interesting finding regarding the unique behavior exhibited by the O^{4+} atom may result from the preferential production of O^{4+} atoms from water cluster species. After the removal of four electrons, the oxygen reaches a closed 1s shell which would require significant additional energy to remove the remaining two valence electrons. Hence, the +4 charge state is the maximum value found in the present experiments.

The Coulomb explosion of water clusters also results in the formation of high energy protons. These protons are indistinguishable within a water monomer. By contrast, the production of high energy protons from methanol clusters yields two types of protons: ones originating from methyl and hydroxyl groups (in a 3:1 ratio). Each proton is sensitive to the charge state in its local environment and each type of proton is expected to behave differently, on average, and exhibit marked differences compared to those from the water system. This paper explores the differences in the types of protons generated from the differing hydrogen bonded clusters.

2. Experimental

For a more complete discussion of the experimental apparatus, refer to ref. [12]. Briefly, methanol clusters were generated via supersonic expansion of room temperature water vapor seeded in helium at a pressure between 1.7 and 2.4 bar. The molecular beam produced in this fashion was first skimmed, and then subjected to ionization with femtosecond laser pulses which were directed to intercept clusters located between the time-of-flight grids; see Fig. 1. Under typical operating conditions, the potential applied to TOF_1 is between 4 and 5 kV while the potential applied to TOF_2 is roughly 3 kV. For the studies presented in this manuscript, TOF_2 was kept constant at a potential of 2982 V and the potential of TOF_1 was systematically varied. The reflectron is held at a constant potential and acts as an ion mirror for ions of a prescribed energy

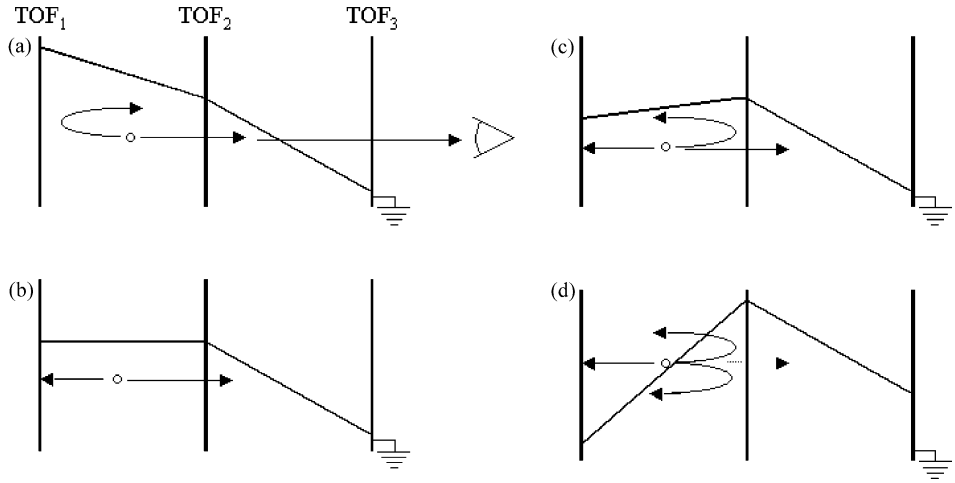

Fig. 1.

range. Those ions with kinetic energy less than the potential of the reflectron are turned toward the detector while those of greater energy are not and hence remain undetected. The detection scheme employs a pair of microchannel plates in a Chevron alignment coupled to an oscilloscope (Agilent Technologies 54820A). Ionization and Coulomb explosion is achieved with an amplified colliding pulse mode-locked ring dye laser (CPM) having an output wavelength centered at 620 nm. The laser is focused between the first two acceleration grids of the mass spectrometer with a 40 cm optical lens, to yield a final focused beam diameter of $\sim$4 μm with peak powers of $\sim 10^{16}$ W/cm^2.

3. Results and discussion

3.1. Experimental findings

A determination of the kinetic energy released from Coulomb explosion events generated in water clusters was achieved using a recently developed method called time-of-flight (TOF) gating. The same general method is employed in the present study of methanol clusters. In the usual TOF mass spectrometer configuration situated for the detection of cations, TOF_1 is placed at a positive potential higher than that of TOF_2 and a grounding grid is located before the field free region as in Fig. 1a. This allows all cations to be accelerated towards the reflectron and then to ultimately impact on the detector. Those ions that have energy less than the repelling grid of the reflectron are detected, while those ions with higher energy than the reflectron maintain a straight trajectory and are not detected. TOF gating employs a method whereby the potential placed on TOF_1 is systematically reduced while all other potentials (TOF_2, the ground potential applied to TOF_3, as well as the reflectron and MCPs) remain constant. As TOF_1 is reduced, a situation arises where the potentials are equal on both TOF_1 and TOF_2. See Fig. 1b. As shown in Fig. 1c, eventually, the potential applied to TOF_1 becomes lower than that of TOF_2, producing a field in the opposite direction than necessary for detecting cations in the traditional method. By reversing the polarity of TOF_1 and generating a negative potential, the gradient between TOF_1 and TOF_2 can be strongly attractive to cations, actually exceeding in magnitude the field strength between TOF_2 (2982 V) and ground; see Fig. 1d.

Using typical time-of-flight settings (such as those depicted in Fig. 1a) with the reflectron operating as an ion mirror, a cut-off study is performed to determine the birth potential (BP) of the ions. Knowledge of the BP is critical since it yields the birth location of ions

between the TOF grids. Frequently, it is assumed that ions are born centered between the accelerating grids, but this is often not the case. The distance between TOF_2 and the laser/molecule interaction region was calculated as follows from Eq. (1):

$$d = l\left(\frac{BP - TOF_2}{TOF_1 - TOF_2}\right) \quad (1)$$

where d is the distance of the birth location from TOF_2 and l is the total distance between TOF_1 and TOF_2. In the present study conducted on methanol, the distance between the grids is 1 cm and the birth location, d, was 0.31 cm from TOF_2 (the birth location for the water study was 0.36 cm). TOF gating was carried out by stepping down the voltage of TOF_1 by increments of 100 V. Eventually, when TOF_1 is at a lower potential than TOF_2, ions must overcome a positive field gradient in order to be detected. The positive field gradient was determined in accord with the relationship given in Eq. (2):

$$qd\frac{(TOF_1 - TOF_2)}{l} = MEKER \quad (2)$$

where q is the integer charge on the ion and MEKER is the minimum excess kinetic energy required for an ion to be detected. This value corresponds to the KER of the forward ejected ions from the Coulomb explosion. The reflectron was set at a constant potential, U_k, which is determined by Eq. (3):

$$\left(\frac{d}{l}V_{Inc}\right) + TOF_2 = U_k \quad (3)$$

where V_{Inc} is the step size by which TOF_1 is decreased (100 V in these studies) and U_k is the voltage applied to the reflectron. If the magnitude of TOF_2 is subtracted from U_k, the voltage window of the energetic species is obtained. In these studies, a voltage window of 31 V was utilized (a voltage window of 36 V was used in the water studies) and was chosen due to the location of the laser/molecular beam interaction area between the electrostatic TOF grids.

When the electric field gradient between TOF_1 and TOF_2 diminishes to zero as in Fig. 1b, only ions that have additional kinetic energy towards the reflectron are detected. As the potential on TOF_1 is dropped further, the minimum kinetic energy required for an ion to overcome the barrier and be detected is increased. Those ions that are able to escape the acceleration region will be detected unless they are so energetic that they exceed the potential placed on the reflectron.

Methanol clusters were generated as described above to yield mass spectra such as the one shown in Fig. 2. Protonated methanol clusters are observed for sizes of $H^+(CH_3OH)_n$, $n \leq 10$, though larger clusters may fragment and remain undetected. At larger cluster sizes, metastable decay can be seen as secondary peaks that arrive at shorter arrival times. These daughter peaks arise from evaporation of a parent peak in the field free region and continue to drift at the parent velocity until encountering the reflectron electric field where they are turned at lower potentials and arrive at the detector at earlier times. The low-mass, early arrival-time region is displayed in Fig. 2 along with the cluster distribution; the overlap in the arrival time for multicharged oxygen and carbon atoms is seen. The focus of this paper is centered on the protons generated by the Coulomb explosion of two separate hydrogen bonded cluster systems. Hence, the data obtained for the oxygen and carbon fragments is not presented here.

Fig. 3 illustrates the distribution of methanol protons detected at various MEKER values. The abscissa contains the MEKER for an ion to escape the attractive potential gradient and be detected. MEKER values were calculated by Eq. (2) above. The ordinate of Fig. 3 is the percentage of ions with a particular KER range. The inset graph in Fig. 3 is from the same data set, but is rescaled to illustrate the behavior of the proton at various selected values of kinetic energy release. The scales are expanded to display features in the data where very little intensity arises at a particular range of kinetic energy release.

The methanol proton MEKER plot extends to energies beyond 2700 V. The intensity profile climbs in probability, until peaking at the energy range that encompasses 100 V of kinetic energy. The MEKER intensity smoothly tapers off from 108 ± 15.5 V and beyond, until reaching the ~900 V window. The final

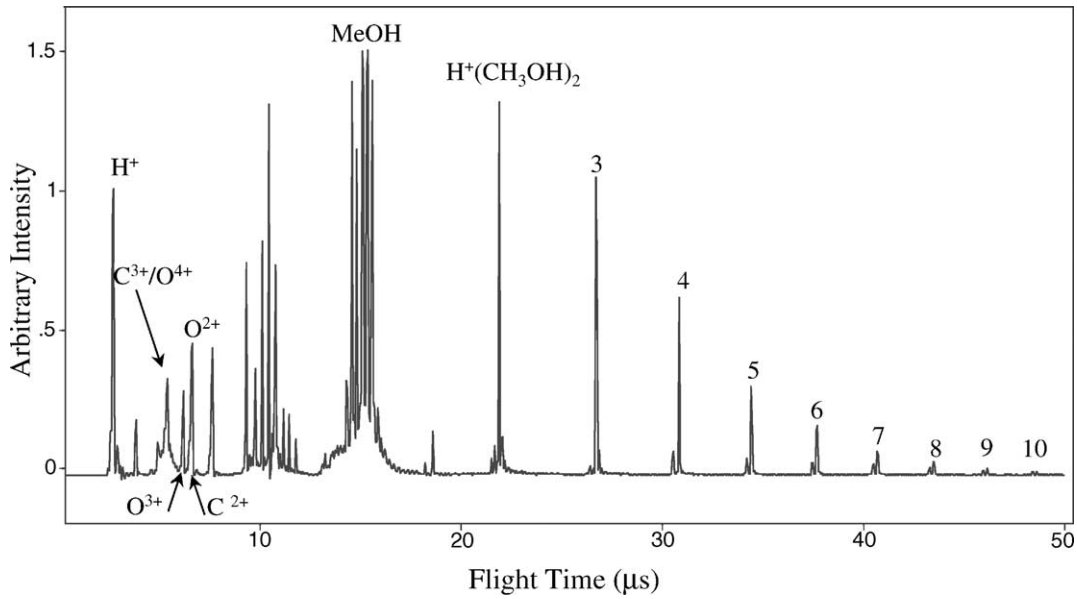
MeOH
H+(CH3OH)2
H+
C3+/O4+
O2+
O3+
C 2+
3
4
5
6
7
8
9
10
Arbitrary Intensity
Flight Time (μs)

Fig. 2.

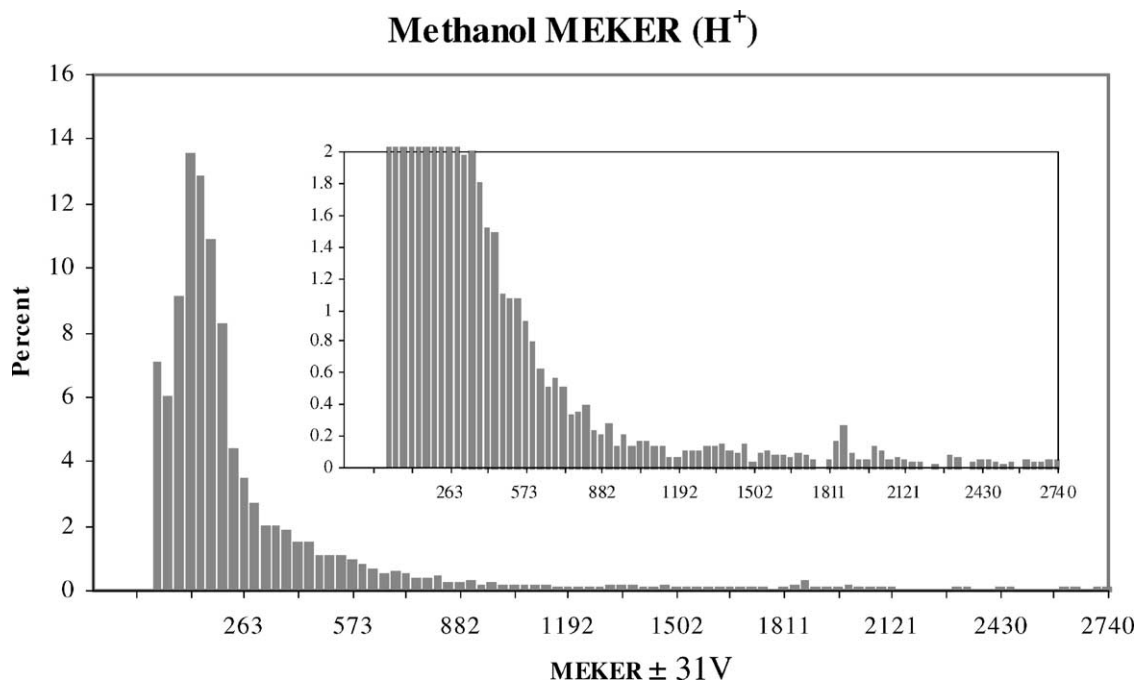
Methanol MEKER (H+)
Percent
MEKER ± 31V

Fig. 3.

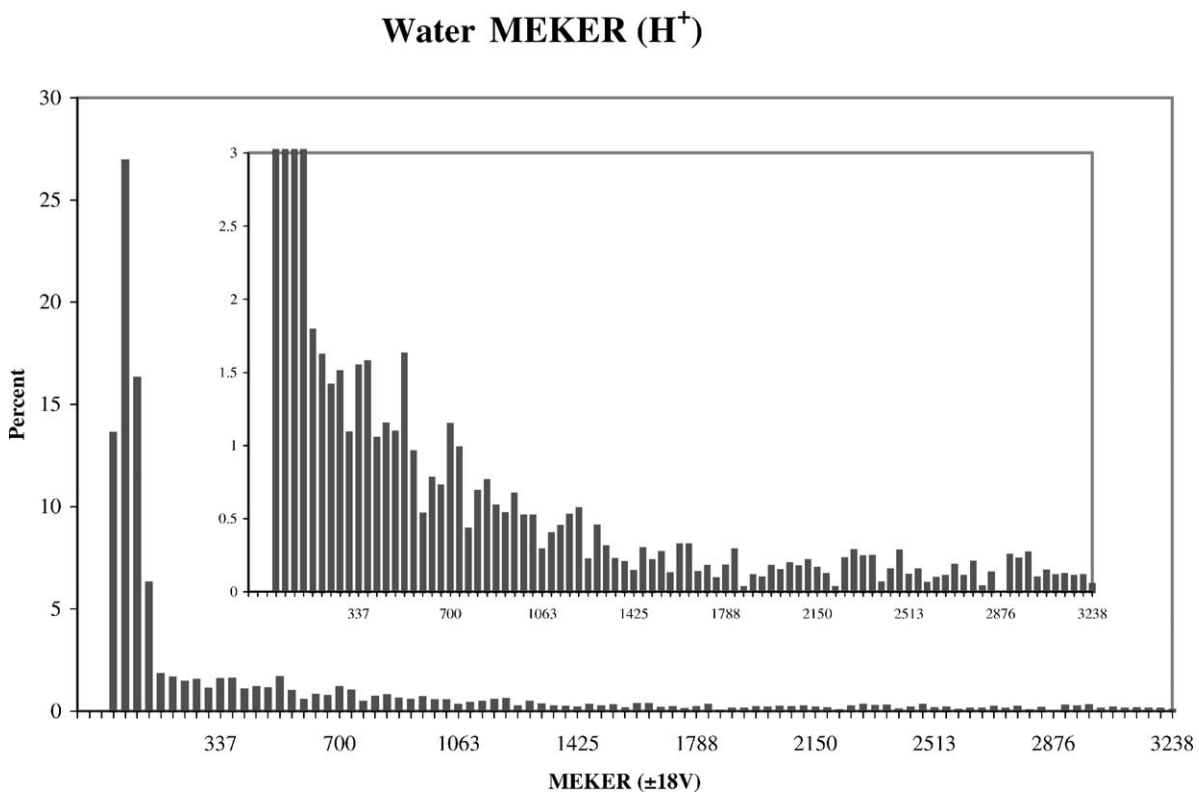

Fig. 4.

region from 900 V to the maximum at 2740 V displays no distinct trend.

An unexpected difference is noted in the proton plots for the methanol cluster series compared to the water cluster series (displayed in Fig. 4 for purposes of comparison). As seen, the water proton plot rises and peaks sharply at about 47 V following zero MEKER, while the methanol proton slowly builds to a maximum at around 100 V as seen in Fig. 3. Furthermore, the insets in Figs. 3 and 4 show that the methanol MEKER population appears to decay more quickly to higher energy ranges than does that of the water proton MEKER.

The average kinetic energy release ⟨KER⟩ determined from the percentage plots for the protons was calculated with Eq. (4):

$$\langle \mathrm{KER} \rangle = \sum_i \left((\mathrm{MEKER})_i \frac{I_i}{\sum_i I_i} \right) \quad (4)$$

where I_i is the peak area associated for a particular MEKER value. The average kinetic energy release calculated for the water protons was 387 V while the average kinetic energy released for the protons in the methanol experiment was calculated to be 265 V.

The clustering in the methanol system is not as extensive in these experiments as for the water studies reported earlier; methanol clusters can be seen out to $n \sim 10$ while, for the water system, clusters were generated to $n \sim 21$. Studies have shown that increased clustering yields both higher charge states as well as higher kinetic energy values [13]. From this general trend, it is understandable that the average kinetic energy release for protons arising from the water cluster system (387 V) is considerably higher than from the methanol cluster system (265 V). However, comparing the methanol system to the water experiments, the data seems contradictory when considering that the methanol plot peaks at a considerably higher value

than that of the water system; the average kinetic energy released in the methanol study is lower than the water study despite the most probable energy for the methanol proton being at 108 V as opposed to 47 V for water. If smaller clusters yield lower average energies, why is the most probable energy range for the methanol system shifted to higher energy relative to the water study? This is likely due to the two different types of protons in the methanol, the hydroxyl and methyl protons. This concept is discussed in detail in the following section on theoretical simulations of a Coulomb explosion event.

3.2. Theoretical findings

A good approximation for kinetic energy release can be deduced through a consideration of Coulomb repulsion using static bond lengths and employing Eq. (5):

$$V = \frac{1}{4\pi\varepsilon_0}\sum_{i\neq j}\frac{q_i q_j}{r_{ij}} \tag{5}$$

where ε_0 is the vacuum permittivity constant, q_i the charge on ion i and r_{ij} is the distance between ions i and j. A series of molecular dynamics simulations were performed to yield the kinetic energy release of each of the fragments resulting from a methanol cluster ($n = 1$–5) employing the method discussed in ref. [14]. This method assumes each atom in the system instantaneously acquires a charge by losing one or several electrons and is used qualitatively to gain insight into the behavior of the cluster fragments.

Assuming a general trend that larger proton energy values arise from clusters in which oxygen is in the +4 charge state, one might expect the hydroxyl protons to be contributing greatly to increased magnitudes of KER due to the closeness to the forcefully repelling oxygen, while the methyl protons might feel less force and acquire less kinetic energy. However, previous studies in our laboratory on mixed water and methanol clusters provide evidence suggesting that while hydroxyl protons participate in hydrogen bonding as expected, methyl groups tend to protrude from the cluster surface [15,16]. It is well established that in the case of closely packed systems, surface ions garner a large portion of the kinetic energy released, suggesting that the methyl protons may contribute more significantly to the energies measured in the present experiments [14]. Moreover, Monte Carlo studies of pure methanol clusters show that methyl groups are located on the outer surface of the cluster [17], further supporting the likelihood that methyl protons are responsible for the larger energies.

In order to further explore these ideas, calculations of KER were performed using the method described by Poth and Castleman [14]. This required information on the locations of the various atoms in the cluster. The molecular structures in Fig. 5 were generated using Gaussian 98 with a STO-3G basis set. While higher levels of theory are available, these simulations served to yield a relatively reliable structure suitable for the generation of Cartesian coordinates required for use in the Coulomb explosion molecular dynamics simulations. The kinetic energies acquired by the various types of protons are summarized in Table 1, where interesting and unexpected findings were

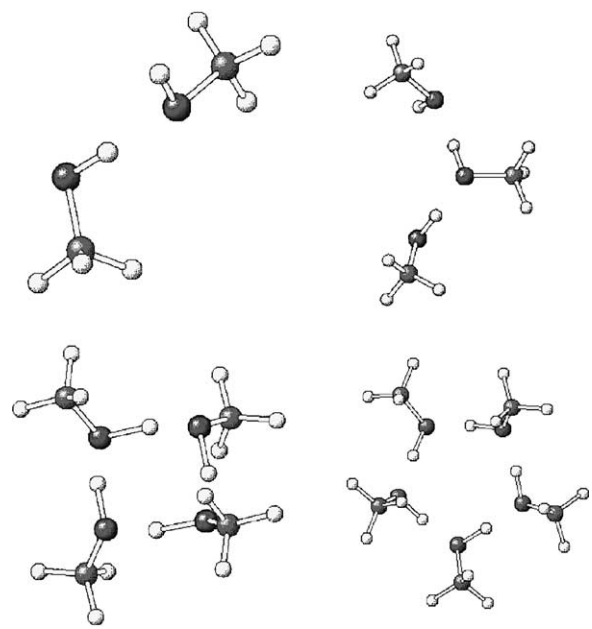

Fig. 5.

Table 1

	Monomer	Dimer	Trimer	Tetramer	Pentamer
Hydroxyl (eV)	91.2	119.2	128.3	201.5	235.6
Methyl (eV)	78.2	112.3	142.1	180.8	194.5

revealed concerning the Coulomb explosion energies arising from the five clusters studied. The simulations were performed by first placing the atoms in the highest charge states observed in the experiments; oxygens were assigned +4 charge states while the carbons were given +3 charge states. The monomer, dimer and trimer structures can be best described as linear while the tetramer and pentamer are ring structures. For the linear structures of the monomer, dimer and trimer, the hydroxyl proton experiences a reversal in the energies obtained by the hydroxyl and methyl protons. For the monomer, the hydroxyl proton obtains 17% more energy than the methyl sibling. For the dimer, the hydroxyl proton continues to garner more energy but the difference diminishes as the hydroxyl proton is only 6% more energetic. The situation reverses for the trimer where the methyl proton acquires more energy. In this third system, the methyl proton obtains 11% more energy. One expects this trend to continue for closely packed clusters [14]. For the ring structures of the tetramer and pentamer, the hydroxyl protons acquire more energy. Considering the findings from these simulations, it can be surmised that densely packed methanol cluster systems lead to methyl protons with larger kinetic energies. In contrast, loosely packed clusters, such as rings that give "hollow" structures, yield energies that are weighted by the hydroxyl species.

For completeness, simulations were also performed for the five clusters with homogenous charge states, that is with each oxygen and carbon in the same +3 charge state. This scenario does not force particular protons to reside next to higher charge states. The findings are summarized in Table 2. The results are strikingly similar to those obtained with oxygen in the +4 charge state and carbon in the +3 charge state. From the homogenous study, it can be surmised that the proton behavior in the methanol study is attributed solely to the bonding structures and not the charge state of the neighbors.

Table 2

	H_h (eV)	H_m (eV)
Monomer	75.6	72.0
Dimer	102.2	101.9
Trimer	109.1	128.5
Tetramer	166.1	163.3
Pentamer	199.8	175.3

Poth and Castleman found that in closely packed systems core species generally obtain less kinetic energy than surface species [14]; therefore, core hydrogens from water clusters would be expected to garner less kinetic energy, thereby leading to a lower most probable energy value. Likewise, core hydroxyl protons from methanol clusters lower the most probable energy range as well. However, considering that there is a 3:1 ratio of methyl to hydroxyl protons, and the methyl protons reside on the surface of the cluster [15,16], the most probable energy range is shifted to higher energy despite a smaller overall cluster distribution for the methanol system.

4. Conclusions

The magnitude of kinetic energy release in Coulomb explosion can extend beyond the capability of the electronics employed in a TOFMS when operating under typical settings. The TOF gating method removes the low or zero kinetic energy ions and slows high energy ions in a controlled manner for facile detection.

The factors contributing to the magnitudes of KER in the case of methanol is somewhat less definitive

than in the water case due to mass overlaps between multicharged carbon and oxygen. On the other hand, focusing on the behavior of the protons does reveal some important and interesting findings. For the proton peak, the average kinetic energy release in the methanol system is considerably lower than those values calculated for the water system. This is likely due to the smaller cluster distribution in the methanol study. Despite the lower average kinetic energy, the methanol system has a larger most-probable window than the water system, a fact which is attributed as being due to the methyl protons that preferentially reside on the surface of the clusters. Comparing experimental measurements with theoretical simulations of larger methanol clusters undergoing Coulomb explosion would be expected to yield useful information regarding the location of multicharged components and their kinetic energy.

Acknowledgements

The authors would like to thank the Department of Energy, Grant No. DE-FG02-92ER14258, for the financial support of this research. The authors would also like to thank T.E. Dermota for generating the structures discussed in the theoretical section of the results and K.L. Knappenberger, Jr. for fruitful discussions.

References

[1] A.H. Zewail, Femtochemistry—Ultrafast Dynamics of the Chemical Bond, vols. I and II, World Scientific, Singapore, 1994.
[2] A.H. Zewail, S. De Feyter, G. Schweitzer (Eds.), Femtochemistry: With the Nobel Lecture of A. Zewail, Wiley-VCH, New York, 2001.
[3] D.E. Folmer, L. Poth, E.S. Wisniewski, A.W. Castleman Jr., Chem. Phys. Lett. 287 (1998) 1.
[4] S. Wei, J. Purnell, S.A. Buzza, E.M. Snyder, A.W. Castleman Jr., in: Manz, Wöste (Eds.), Femtosecond Chemistry, Springer-Verlag, Germany, 1994, p. 449.
[5] S.A. Buzza, E.M. Snyder, D.A. Card, D.E. Folmer, A.W. Castleman Jr., J. Chem. Phys. 105 (1996) 7425.
[6] J. Purnell, E.M. Snyder, S. Wei, A.W. Castleman Jr., Chem. Phys. Lett. 229 (1994) 333.
[7] J.V. Ford, Q. Zhong, L. Poth, A.W. Castleman Jr., J. Chem. Phys. 110 (1999) 6257.
[8] E.M. Snyder, S.A. Buzza, A.W. Castleman Jr., Phys. Rev. Lett. 77 (1996) 3347.
[9] E.M. Snyder, S. Wei, J. Purnell, S.A. Buzza, A.W. Castleman Jr., Chem. Phys. Lett. 248 (1996) 1.
[10] T.D. Ditmire, J. Zweiback, V.P. Yanovsky, T.E. Cowan, G. Hays, K.B. Wharton, Phys. Plasmas 7 (2000) 1993.
[11] T. Ditmire, J. Zweiback, V.P. Yanovsky, T.E. Cowan, G. Hays, K.B. Wharton, Phys. Plasmas 7 (2000) 1993.
[12] E.S. Wisniewski, J.R. Stairs, A.W. Castleman Jr., Int. J. Mass Spectrom. 212 (2001) 273.
[13] D.A. Card, E.S. Wisniewski, D.E. Folmer, A.W. Castleman Jr., J. Chem. Phys. 116 (2002) 3554.
[14] L. Poth, A.W. Castleman Jr., J. Phys. Chem. 102 (1998) 4075.
[15] Z. Shi, S. Wei, J.V. Ford, A.W. Castleman Jr., Chem. Phys. Lett. 200 (1992) 142.
[16] X. Zhang, A.W. Castleman Jr., J. Chem. Phys. 101 (1994) 1157.
[17] D. Wright, M.S. El-Shall, J. Chem. Phys. 105 (1996) 11199.